Wissenschaftliche Gesellschaft Lasertechnik e.V.

Lasers in Manufacturing Conference 2021

Low temperature and high concentration laser doping system for fabrication of 4H-SiC power devices

Toshifumi Kikuchi[a,*], Takuma Yasunami[a], Akira Mizutani[a,b], Daisuke Nakamura[a] and Hiroshi Ikenoue[a,b]

[a]*Grad. Sch. ISEE. Kyushu Univ.,*
[b]*Dept. of Gigaphoton Next GLP, Kyushu Univ.,*
[a,b]*744 Motooka, Nishi-ku, Fukuoka 819-0395, Japan*
Mobile Phone: +81-80-5536-6070

Abstract

We propose a high-concentration and low-crystal-damage doping method by irradiating deposited films with a KrF excimer laser containing dopant atoms on the 4H-SiC surfaces. This laser doping method is a low-temperature process that reduces the thermal stress on the substrate, and it can achieve a doping concentration of ~10^{20} cm^{-3} or higher, which exceeds the limit of the ion implantation method.
In this study, we investigated the peak energy dependence of the crystal damage and surface roughness by controlling the pulse width of the laser for doping. It was found that the crystal damage and surface roughness were reduced by suppressing the peak energy. In addition, we report on the construction of a laser doping system to improve the compatibility with the manufacturing process of 4H-SiC power devices.

Keywords: laser doping, power device, semiconductor, excimer laser, 4H-SiC;

1. Introduction

4H-silicon carbide (4H-SiC) is a wide-bandgap semiconductor with excellent material properties and is used as a material for power devices and devices for environmental applications. Currently, schottky barrier diodes (SBDs) and metal-oxide-semiconductor field-effect transistors (MOSFETs) mass-produced and distributed on the market [1,2].

* Corresponding author.
E-mail address: kikuchi@ees.kyushu-u.ac.jp

In contrast, the process technology for 4H-SiC devices has several issues, such as defect reduction during wafer manufacturing and impurity doping. The ion implantation method is widely used for impurity doping. However, the high-temperature process at the time of activation annealing at approximately 1700 °C limits the manufacturing process [3,4]. Therefore, for the p-type and n-type of the surface device structure, a method of using epitaxial growth are used [5]. In the contact electrode formation process on the back surface, a method was used in which Ni was formed and furnace annealing was performed at approximately 1000 °C are used to reduce the contact resistance. However, this method involves a high process temperature; hence, a method of replacing the furnace annealing process with laser annealing has been studied [6,7]. This method relies on carrier generation by introducing carbon defects, and is limited to increasing the density of carriers. Therefore, the stable contact resistance value is limited to the first half of 10^{-5} Ωcm^2. In addition, carbon clusters generate at the Ni/4H-SiC interface owing to the formation of carbon defects, which causes electrode peeling. In our previous study, we achieved high-concentration nitrogen doping and n-type characteristics by forming Si_xN_x as a film containing a dopant on 4H-SiC and irradiating it with a laser [8]. In this study, we conducted 4H-SiC surface roughness measurement and cross-sectional transmission electron microscopy (TEM) analyses by doping with various laser pulse widths to evaluate the surface condition of 4H-SiC doped with a high concentration of nitrogen. The crystalline state after laser doping is important for stable properties, and the surface roughness affects device fabrication, such as electrode peeling. In this study, to analyze the contact resistance, surface roughness, and other factors, which are important for device performance, we created a test chip with an accuracy of 1 µm and evaluated the contact resistance at x 10^{-6} Ωcm^2 using our own calculation method.

2. Experimental

2.1. Experimental conditions

Figure 1 shows a schematic of the laser irradiation and roughness analysis system. Laser irradiation was performed using a KrF excimer laser (Gigaphoton Inc., wavelength: 248 nm). The pulse width could be selected from approximately 26 ns, 47 ns, and 82 ns by delaying the light using an optical system. The repetition frequency was set from 1 to 4000 Hz. In this experiment, we set it to 100 Hz. The laser beam was cut out near the center using an aperture with a size of 300 µm × 400 µm on the sample surface. The XY stage had a maximum speed of 300 mm/s. In this experiment, the stage speed was set to 4 mm/s, and the number of laser irradiations was set to 10 shots/loc. To reduce the oxidation in the area irradiated by the laser, the procedure was performed in an Ar atmosphere using a gas supply nozzle. The surface roughness after laser irradiation was obtained using a 3D laser microscope (height resolution of 0.5 nm). The sample structure was a Si_xN_x (100 nm)/n-type 4H-SiC(0001) substrate. The Si_xN_x film was deposited on the C-face of the 4H-SiC substrate via chemical vapor decomposition. During laser doping, the irradiation fluence was set to 1.8–3.8 J/cm^2 and laser irradiation was performed. After irradiation, the Si_xN_x film was removed with hot phosphoric acid at 150 °C, while the carbon-based and silicon-based products were removed by O_2 and CF_4 plasma etching.

2.2. Contact resistance measurement method

Figure 2 shows the structure of the test chip used to measure contact resistance. In the region doped with a high concentration of nitrogen by laser irradiation, a contact holes "d" with different sizes were formed in the SiO_2 insulating film with an accuracy of 1 µm using the photolithography method. For the contact resistance on the side opposite to laser doping, Ni was deposited in the first step and the furnace was annealed

at 850 °C for 30 min to lower the contact resistance and form ohmic contacts. Therefore, the contact resistance value can be obtained using equations (1), (2), and (3) by changing the contact area "d x d" between the electrode and the semiconductor.

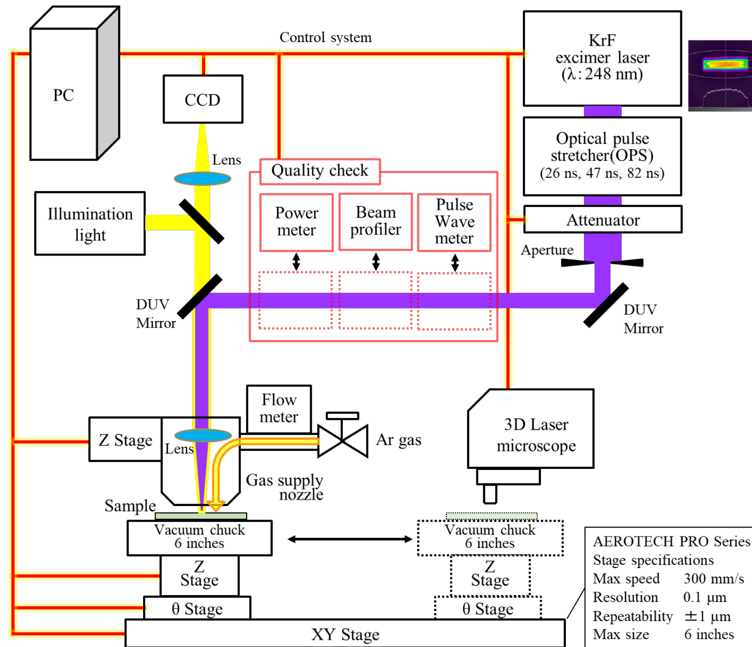

Fig. 1. Schematic of the laser irradiation system.

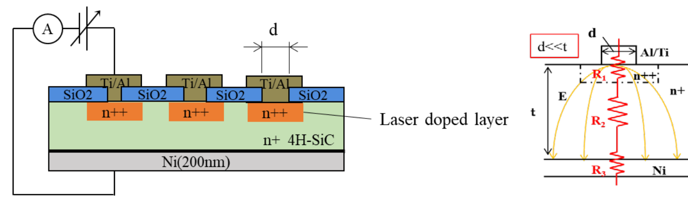

Fig. 2. Structure of test tip for contact resistance measurement and contact resistance calculation method

$$R_M = R_1 + R_2 + R_3 \quad (1)$$

$$R_1 = \rho_C / d^2 \quad (2)$$

$$R_M = \rho_C / d^2 + R_2 + R_3 \quad (3)$$

3. Results and Discussion

3.1. Contact resistance and surface roughness evaluation

Figure 3 shows the contact resistance and surface roughness after laser irradiation and compares the results with pulse widths of 46 and 82 ns. Comparing the contact resistance values by pulse width, in the case of a pulse width of 46 ns, the fluence was 2.4 J/cm^2 and the contact resistance was 1.92 x 10^{-6} Ωcm^2, which was the lowest value. In the case of a pulse width of 82 ns, the fluence was 3.0 J/cm^2 and the contact resistance was 1.3 x 10^{-6} Ωcm^2, which was the lowest value. There is a dependency between the fluence and contact resistance, and as the fluence is increased from the fluence value at which the contact resistance is lowered, the value of contact resistance increases gradually. This effect was particularly pronounced for a pulse width of 46 ns. An excessively high value of fluence is not suitable for lowering the contact resistance. The surface roughness also tended to increase with a pulse width of 46 ns. Lower fluence can not obtain high concentration doping. Higher fluence causes increase surface roughness which is not good for lowering the contact resistance. The surface roughness (arithmetic mean roughness) was 9.6 nm with a pulse width of 46 ns and 3.2 nm with 82 ns at 2.4 J/cm^2, respectively. Low fluence is effective for low surface roughness and low contact resistance from around 82 ns pulse width.

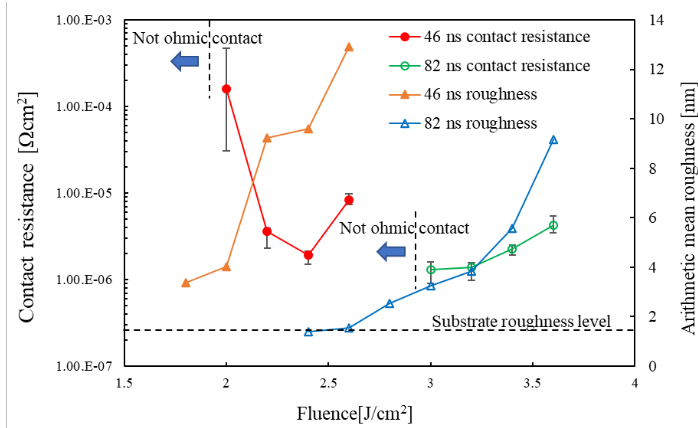

Fig. 3. Fluence and pulse width dependence of contact resistance and surface roughness

3.2. Evaluation of crystal state after laser irradiation

Figure 4 shows cross-sectional TEM images and electron diffraction patterns of the laser-irradiated 4H-SiC, which showed lowest contact resistance with pulse widths of 46 ns and 82 ns. At each pulse width, the 4H-SiC structure is maintained after laser irradiation. Under the pulse width of 82 ns in Fig.4 (b), the electron diffraction pattern is confirmed more clearly. The obscuration in Fig.4 (a) is due to the distortion caused by some partial defect formation as shown by the arrow. The ratio of elements was measured using energy dispersive X-ray spectroscopy, and the values were close to those of non-irradiated 4H-SiC under each pulse width (Table.1). The reason for the slight change in the Si and C composition ratio is that the EDX spectrum

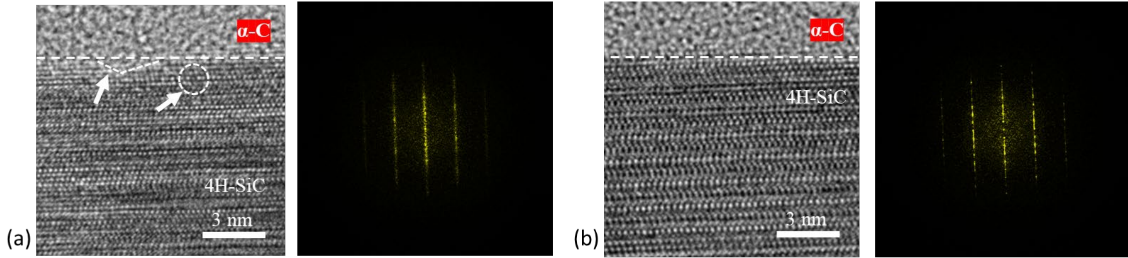

Fig. 4. Cross-sectional TEM images and electron diffraction patterns, where (a) a pulse width of 46 ns and fluence of 2.4 J/cm^2 and (b) a pulse width of 82 ns and fluence of 3.0 J/cm^2.

indicates the presence of nitrogen, and the C and O spectra increase in proximity to the nitrogen detection spectrum.

Figure 5 shows the cross-sectional TEM image and electron diffraction pattern of a pulse width of 82 ns and fluence of 3.8 J/cm^2. From this figure, the 4H-SiC crystal state is altered by a very high fluence. It is known that 4H-SiC becomes 3C-SiC- or Si-based by melting and recrystallization, and this was confirmed in our laser irradiation experiment. From the electron diffraction pattern, a structure closer to the Si crystal was confirmed. In addition, the composition ratio was different between the black distorted region and the other regions in the TEM image in Fig. 5 (a), and carbon defects generated that occurred during the high-temperature processing of 4H-SiC were also confirmed (Table.1). The surface roughness is correlated with the crystal state caused by laser irradiation, and if the crystal state is heavily disturbed, the surface will be extremely rough.

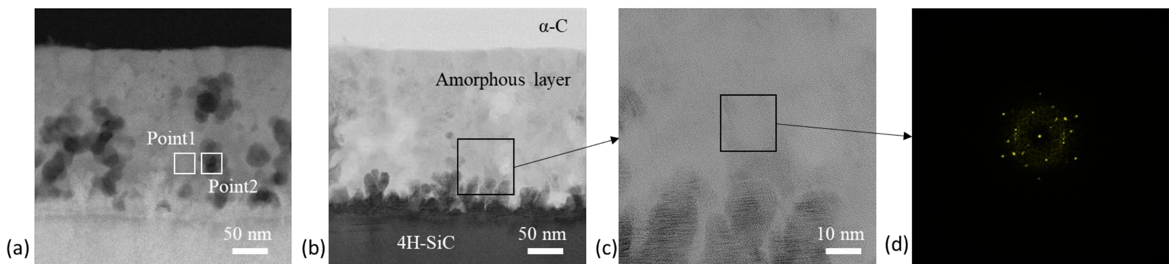

Fig. 5. Cross section TEM images and Electron Diffraction pattern of excessive fluence condition (A pulse width of 82 ns and fluence of 3.8 J/cm^2)

Table. 1 Energy dispersive X-ray spectroscopy analysis for each laser irradiation condition

Pulse width	Non-irradiation	46 ns		82 ns	
Fluence	Non-irradiation	2.4 J/cm^2	3.0 J/cm^2	3.8 J/cm^2 Fig.5(Point1)	3.8 J/cm^2 Fig.5(Point2)
Element	Composition (Atomic %)				
Carbon	51.1	55.1	56.1	34.0	88.3
Silicon	47.7	43.8	42.6	63.4	11.0
Oxygen	1.2	1.1	1.4	2.7	0.7

3.3. Depth of nitrogen diffusion by laser doping

Figure 6 shows the results of secondary ion mass spectrometry (SIMS) analysis for the two conditions that showed low values of contact resistance. In both cases, it can be confirmed that a high nitrogen concentration in the range of 10^{21} cm^{-3} was achieved in the surface layer. The contact resistance value of 1.3 × 10^{-6} Ωcm^2 obtained in this study can be attributed to the dominance of the tunneling effect at an activation concentration of 1 × 10^{20} cm^{-3} or higher. Therefore, nitrogen diffusion and activation were achieved simultaneously by laser irradiation. As for the diffusion depth, it was confirmed that the surface concentration remained the same, but the diffusion depth was 10 nm greater in the 82 ns condition than in the 46 ns condition while maintaining a high concentration on the surface.

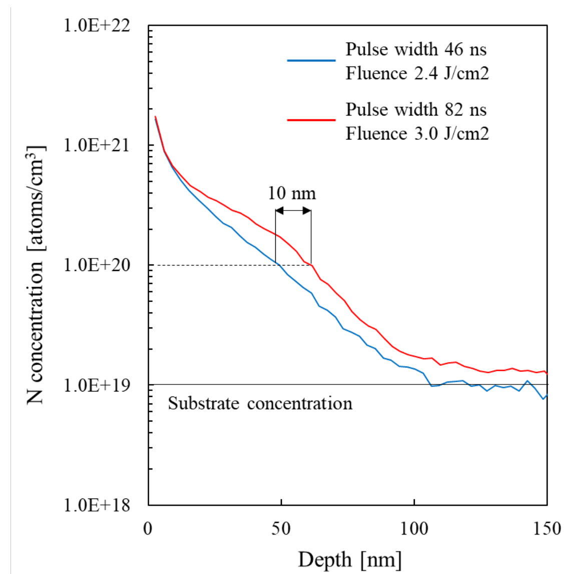

Fig. 6. SIMS depth profiles of N obtained from the laser doping

3.4. Discussion

From these results, for a pulse width of 46 ns, a low contact resistance was obtained, but the surface roughness was approximately 9 nm, whereas for a pulse width of 82 ns, the surface roughness can be reduced to approximately 3 nm with a low contact resistance, indicating that both the fluence and peak pulse power affect the crystal state. In the case of the 82 ns pulse width, the low contact resistance and low surface roughness were maintained even when the fluence was increased compared to the pulse width of 46 ns, and the change in the crystal state due to fluence was suppressed. The SIMS analysis results showed that the difference in contact resistance at each pulse width even with the same nitrogen concentration was probably due to the difference in the activation rate, and maintaining the crystallinity is important for forming a low contact resistance. Therefore, in laser doping, the pulse width is an important parameter for maintaining crystallinity and is necessary to achieve a low contact resistance and low surface roughness.

4. Conclusions

We achieved a contact resistance of 1.3 $\times 10^{-6}$ Ωcm^2 and a surface roughness of approximately 3 nm in the 4H-SiC device fabrication process using an excimer laser pulse extension technology (OPS) with a pulse waveform of 82 ns, which is compatible with the laser doping production line. Using a pulse width of 82 ns, the process margin was also 3.0–3.2 J/cm^2, indicating high process adaptability. Laser doping achieved a contact resistance that was one order of magnitude lower than that of the competing process of Ni deposition followed by annealing, which relies on carrier generation by introducing carbon defects. The good crystalline condition of laser doping is also expected to improve the yield of the manufacturing process. Laser doping technology has shown the possibility of controlling the activation rate and diffusion depth by changing the pulse width further and is expected to be applied as a doping method for surface device processes and p-type formation in the future.

Acknowledgements

We express our sincere gratitude to the staff of Tamari industry for their cooperation in the fabrication of the laser irradiation system, and to the staff of the New Industry Creation Hatchery Center of Tohoku University for their technical cooperation in the semiconductor process and the equipment provided.

References

[1] M. Treu., R. Rupp., and G. Sölkner., 2010. Reliability of SiC power devices and its influence on their commercialization - review, status, and remaining issues," 2010 IEEE International Reliability Physics Symposium, 2010, pp. 156-161.

[2] Kenji Hamada., Shiro Hino., Naruhisa Miura., Hiroshi Watanabe., Shuhei Nakata., Eisuke Suekawa., Yuji Ebiike., Masayuki Imaizumi., Isao Umezaki., and Satoshi Yamakawa., 2015. 3.3 kV/1500 A power modules for the world's first all-SiC traction inverter, Jpn. J. Appl. Phys. 54 04DP07.

[3] D. Peters., R. Schorner., K. H. Holzlein., and P. Friedrichs., 1997. Planar aluminum-implanted 1400 V 4H silicon carbide p-n diodes with low on resistance, Appl. Phys. Lett. 71, 2996.

[4] Carl-Mikael Zetterling., 2002. Process Technology for Silicon Carbide Devices, INSPEC, London, 5.

[5] K. Fukuda et al., 2015. Development of Ultrahigh-Voltage SiC Devices, in IEEE Transactions on Electron Devices, vol. 62, no. 2, pp. 396-404.

[6] R. Rupp., R. Kern., and R. Gerlach., 2013. Laser backside contact annealing of SiC power devices: A prerequisite for SiC thin wafer technology, International Symposium on Power Semiconductor Devices & IC's (ISPSD), 2013, pp. 51-54.

[7] Karim Huet., Fulvio Mazzamuto., Toshiyuki Tabata., Ines Toqué-Tresonne., Yoshihiro Mori., 2017. Doping of semiconductor devices by Laser Thermal Annealing Materials Science in Semiconductor Processing Volume 62, Pages 92-102.

[8] T. Kikuchi., K. Imokawa., A. Ikeda., D. Nakamura., T. Asano., and H. Ikenoue., 2019. Low-temperature, high-concentration laser doping of 4H-SiC for low contact resistance, Proc. SPIE 10905, Laser Applications in Microelectronic and Optoelectronic Manufacturing (LAMOM) XXIV, 109050Z